Turkish Journal of Engineering

https://dergipark.org.tr/en/pub/tuje

e-ISSN 2587-1366

Design and manufacture of the Torque test setup for small and shapeless materials

Zeliha Coşkun*[1], Talip Çelik[1], Yasin Kişioğlu[1]

[1]*Kocaeli University, Faculty of Technology, Department of Biomedical Engineering, Kocaeli, Turkey*

Keywords
Torsion test setup
FEA
First metatarsal
Bone PLA

ABSTRACT

In this study, the design and manufacture of torque test set up has been carried out for small and shapeless speciment. The torque sensor, which has maximum 10 Nm, is used in the test system design. The certain specification of Nema 34 step motor which use to apply torsional force to the specimens is 12 Nm, 24V and 4.2 ampere. The step motor is controlled by the HY-DIV268N-5A Step Motor Driver and the supply voltage of driver is 24 Volts. The information about the degree of the specimen rotation was taken from potantiometer. The information obtained from the sensor and potentiometer was transferred to the LabVIEW software to be representation graphically using the USB 6003 DAQ card. The first metatarsal bone modelled from computerized tomography (CT) images was produced by Ultimaker2 3D printer using polylactic acid (PLA) material. The printed bone model was tested through torsion test set up. At the same time, the 3D bone was prepared for finite element analysis. Boundary conditions were applied in the finite element analysis (FEA) model in accordance with the test setup. The produced bones using 3D printer were subjected to torsion test with the test setup. Also the modelled bone was tested in accordance with the torsion test setup by using finite element analysis. After that, the FEA and experimental test results were compared with each other. As a conclusion, the optimization of the torsional test setup was performed based on the FEA.

1. INTRODUCTION

The rotational force on an axle or the system that creates the rotational force is defined as torque. The unit of torque is the expression of the weight created by the rotational force at the end of the one meter arm in newtons. Torsion occurs when the twisting moments are applied to the rod [Wu et al. 2020]. Torsion is induced by pair of forces and these forces act in two separate planes perpendicular to the axis of the rod [Murakami 2019]. Torsion testing helps to determine the torsional strenght of the materials. Torsion testing is a way of determining how an object will react during normal operation or when bent deliberately until it breaks. Static torque measurement is increasingly used by manufacturers as a method of quality control to comply with industry standards [Abutahoun et al. 2018]. It ensures the proper functioning of components and helps to research their safety and fitness for purpose. It could be useful identify the cause of various defects to reduce costs and increase efficiency. Many products and components, even parts of the body, are subjected to torsional forces during their routine activities [Rohlmann et al. 2014]. In addition to many products such as switches, fasteners, torsion testing is frequently applied to test biomedical equipments. The measurable values with torsion test include; the yield-shear strength, modulus of elasticity in shear, torsional fatigue life, ductility, ultimate shear strength, and modulus of shear [Traphöner et al. 2018]. The torsion test gives highly decisive results in order to control the design of the product, increase the quality and provide that it is produced correctly. Torsion test frequently preferred in biomedical applications and is used in the mechanical evaluation of invasive and noninvasive materials [Sykaras et al. 2000]. It is one of the frequently used mechanical tests in suitability evaluations in artificial organ/tissue or limb studies [Dahl et al. 2018, Fatihhi et al. 2016, Varghese et al. 2011, Kasra and Grynpas 2007]. Additionally it supplies values that can be taken as a reference in the follow-up of the healing process in orthopedic treatments [Kumar et al. 2020]. The soft tissues and bones in the body could

* **Corresponding Author**

*(zeliha.coskun@kocaeli.edu.tr) ORCID ID 0000– 0001 – 6901 – 3465
(talip.celik@kocaeli.edu.tr) ORCID ID 0000 – 0003 – 0033 – 2454
(ykisioglu@kocaeli.edu.tr) ORCID ID 0000 – 0002 – 9819 – 2551

Cite this article

Coskun Z, Celik T & Kisioglu Y (2022). Design and manufacture of the Torque test setup for small and shapeless materials. Turkish Journal of Engineering, 6(1), 81-86

Research Article / DOI: 10.31127/tuje.843320

Received: 19/12/2020; Accepted: 25/03/2021

experience torsional forces during daily routine. The soft tissues have higher torsional strength thanks to their flexibility than bone tissue [Kaur and Singh 2019]. Therefore, it is essential to calculate the torsional resistance of bone tissue. In the literature, there are more studies examining the mechanical properties of long bones such as femur and tibia than studies on short bones [Kumar et al. 2020, Kirthana et al. 2020, Kuwashima et al. 2019, Wahab et al. 2020]. There are difficulties in finding the required test setup for the research to eliminate such deficiencies. On the other hand, there are problems about the suitable clamp design for objects that do not have a smooth shape such as bones. For this reason, the bone tips are frozen with various chemicals and these parts are attached to clamps [Ağın et al. 2019]. Another problem is to freeze the bone specimens at the proximal and distal ends without an axis shift.

The aim of this study is to design and manufacture a torsion test setup for short bones and offer solutions to mentioned above problems. Torsion test was performed with experimental and computer-aided finite element analysis (FEA) analysis after design and manufacture. The experimental and FEA results were compared in order to optimize of the test setup. As a result of various difficulties experienced in the study, various optimizations were carried out in the test setup.

2. METHOD

2.1. Experimental System Design

2.1.1 Mechanical Design and Manufacture

Firstly, the torque sensor, reducer and stepper motor in real dimensions were modeled using SolidWorks. The other parts of the test setup were designed to fit these parts as seen in Figure 1. The torque sensor and the clamp on the sensor tip could be mounted perpendicular to the sigma profile due to the support part. The sensor was fixed to the support part with screw holes. The clamps were designed to fix the bone specimens at proximal and distal ends. One of the clamps was placed on the sensor and the other is placed on the reducer. The potantiometer was placed on the reducer via the gear mechanism order to raise the reducer to sensor level, a rectangular part was designed and located on the bottom of the reducer. The torsional test set up was fixed on the sigma profile.

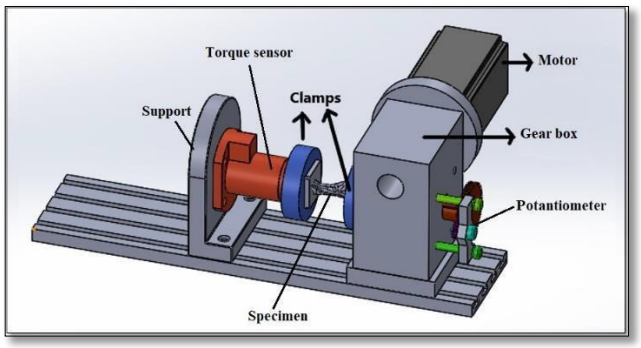

Figure 1. The design of the torional test set up

After the designing and FEA stage, the production stage of the designed parts was started. In order to place the bone specimen easily, the torque sensor side of the test setup was mounted as movable. The production was carried out with Ultimaker2 3D printer using PLA material. The parts were produced at high infill density in order to avoid any problems about the mechanical strength during the experiment. The produced parts were assembled on the sigma profile and the bone was placed between two clamps and subjected to torsion test as seen in Figure 2.

Figure 2. Torsional test setup

2.1.2 DAQ Design

2.1.2.1 Torque Measurement

PCE-FB10TW torque sensor, which is maximum capacity of 10 Nm, was used in the system design. The sensor was fixed perpendicular to the sigma profile with the support. The clamp was attached to the sensor. The support and the clamp were produced with 3D printer from PLA.

Nema 34 step motor, which is the maximum capacity of 12 Nm was used to apply torsional force to the bone specimens in the system design. The step range of the stepper motor was reduced from 1.8 to 0.225 using HY-DIV268N-5A Step Motor Driver. Therefore, the sensitivity of step range were increased. The supply voltage of the stepper motor is 24 V and it was controlled by Ardunio Uno.

2.1.2.2 Position Measurement

The information about the rotational degree of the bone specimens was taken from the potentiometer. Since the potentiometer does not work completely linear, the linear region of the potentiometer was determined by performing the experimental study. The angle information was received and recorded by the Labview software. The potentiometer works linearly between 20-250 degrees according to the experimental study as seen in Figure 3. The angle sensitivity of the potentiometer which is used in this range was increased by using 1/4 gear mechanism. In order to determine the angle precision, the clamp is divided into 360 sections. The rotation angle of the clamp was determined over these sections.

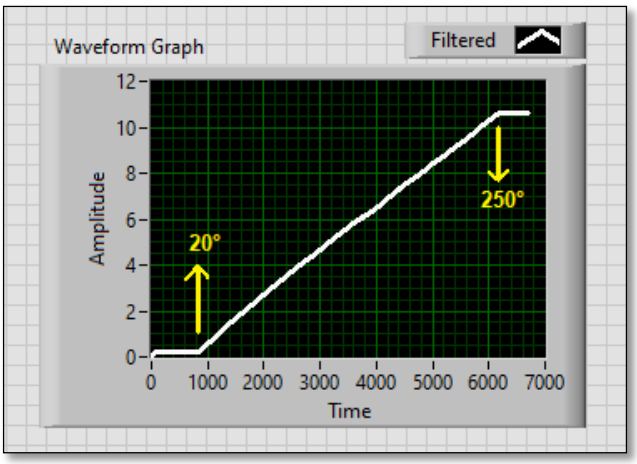

Figure 3. Linear working region of the potentiometer

2.1.2.3 Software Details

The torque and angle information from the sensor and the potentiometer were transferred to the Labview program, respectively, using a USB-6003 DAQ card. USB 6003 is a multifunctional device used in applications such as simple data logging (Figure 4). It offers analog and digital input/output. USB 6003 card is communicate with the computer via the USB port. It allows us to transfer the analog data that receives from the sensor and potentiometer to the Labview program. Labview software works on the basis of graphical representation. A graph was obtained by using torque and position information taken from the sensors. The position and torque information was transferred to the x and y axes, respectively.

Figure 4. USB 6003 DAQ Card

2.1.3 Sample Preperation

2.1.3.1 CAD Modeling

The first metatarsal bone was modeled from computerized tomography (CT) images in Digital Imaging Communications in Medicine (DICOM) format using the MIMICS 12 (Materialise, Leuven, Belgium) 3D Image Processing Software program (Figure 5). The surface defects in the modeled bone were corrected by using Geomagic Studio 10 software (Raindrop Inc., USA).

2.1.3.2 *3D Printing*

After the model corrected, it was transferred to SolidWorks program in IGES format. The bone model that was converted to stl format was transferred to the Ultimaker Cura Software to create g-code. G-code is used in computer-aided manufacturing techniques. The bone models have printed in %100 infill density from PLA material by using Ultimaker2. Since the bone specimens are shapeless, they were molded at proximal and distal ends with the casting type polyester resin, in suitable sizes for clamps. The mold used for this purpose was designed and produced from PLA material with an inner size of 40x40 mm. An adjustable gripper was used to hold the bone in the same position during the freezing process as seen in Figure 6.

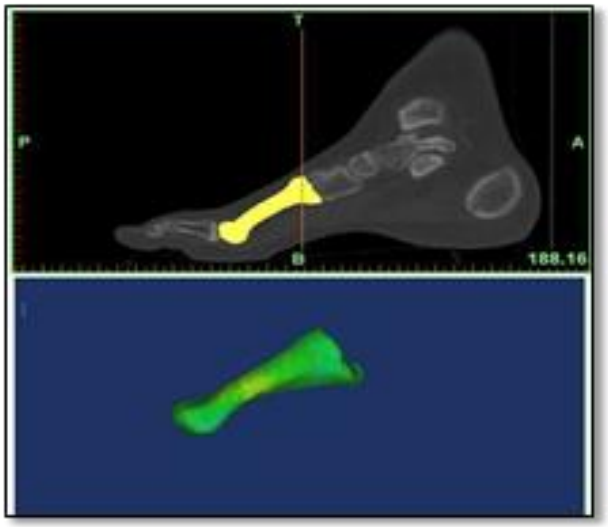

Figure 5. Modelling of the first metatarsal bone

Figure 6. Molding of first metatarsal bone

2.2. Finite Element Analysis

To simplify the analysis, the finite element model was created just for the clamps, the molding parts and the bone as seen in Figure 7. The material properties of the clamps and the bone specimen were defined as PLA and the molding parts were described as the resin material. The elasticity modulus and poisson ratio of the PLA is 3200 MPa and 0.3, respectively. The yield strength of the PLA is 35.9 MPa [Kaygusuz and Özerinç 2019].

Additionally, the elasticity modulus and poisson ratio of the resin is 3800 MPa and 0.3, respectively. The resin material has a tensile strength of 70 MPa. The contact types were described as frictional between the molding parts and clamps. The frictional coefficient was defined as 0.2 [Çelik et al. 2017]. The other contacts were designated as bonded. For the boundary conditions, one of the clamps was fixed from the screw holes and the torsion of 6 Nm was applied to the other clamp.

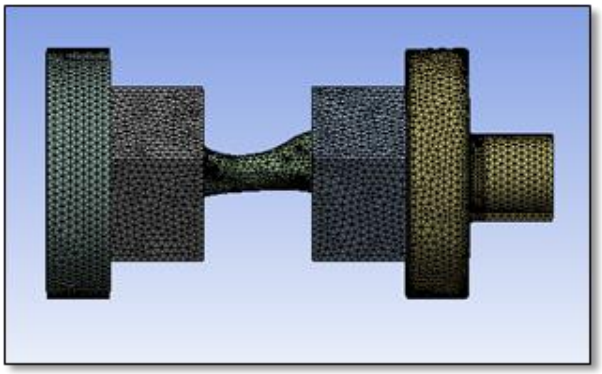

Figure 7. FEA model

3. RESULTS and DISCUSSION

According to the finite element analysis performed on the designed experimental setup, it was observed that when 6 Nm of torque was applied to the bone sample, a 56.4 MPa equivalent (von-Mises) stress occurred on the bone (Figure 8). Because the maximum tensile strength of the bone material is 48 MPa, this stress value will damage the bone. Besides, it was observed that the equivalent (von-Mises) stress value of 16 MPa occurred in the clamps (Figure 9). According to this stress value, it is predicted that there will be no damage to the clamps. The resulting equivalent (von-Mises) stress value for the resin material is calculated as 36.4 Mpa (Figure 10).

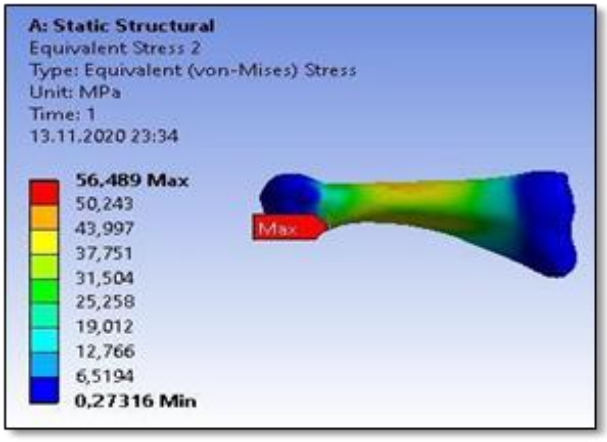

Figure 8. Stress distribution on the modelled bone

This value is below the maximum tensile strength value of the resin material, 70 MPa, and therefore no damage is expected in this material. According to the results of the analysis, only the damage was seen in the bone, and this situation showed that the torsion test achieves its purpose. Thus, it has been observed that the designs and the selected materials are suitable for the test setup.

After the assembly of the produced test setup parts, the bone specimen was placed in the torsion test setup. In the torsion test performed, the plastic deformation of the bone sample has started at 5 Nm. This result showed that the FEA result is accurate. The angle of twist in the bone model was calculated as 16.7 degrees with the FEA. In the experimental study, the twisting angle of the bone model was determined as 24.8 degrees. The difference between the experimental and FEA results is due to the fact that the molding parts and clamps do not overlap each other during the experimental study. When the bone specimen was started to be rotated, the twisting angle shift has occurred due to the gap between the molding part and the clamp. To prevent this, the molding part and the clamps were fixed to each other with the help of a rod by drilling holes with a drill.

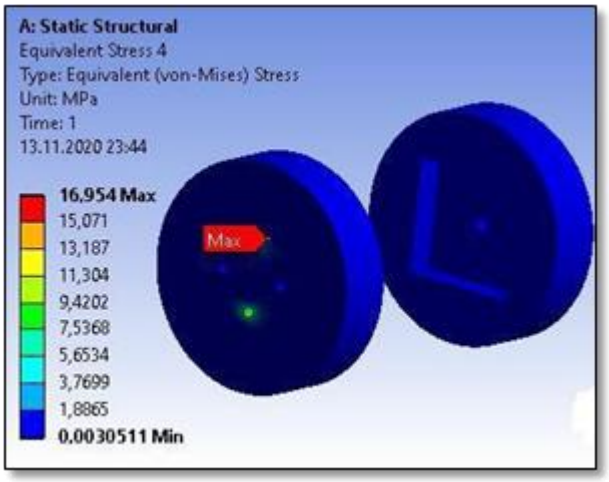

Figure 9. Stress distribution on the clamps

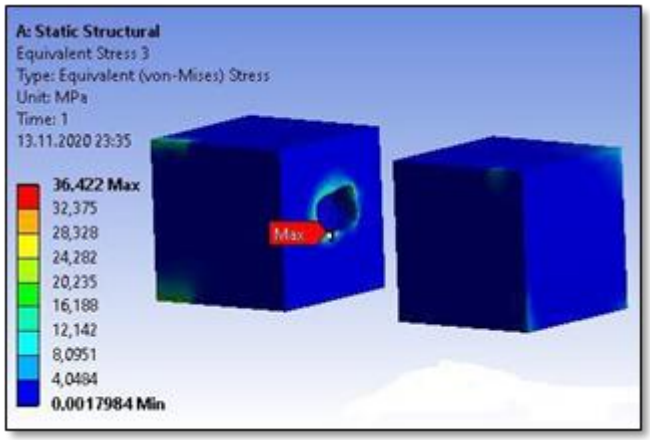

Figure 10. Stress distribution on the molding parts

The graphical representation of experimental and FEA results were determined in Figure 11 and Figure 12, respectively. Figure 11 was obtained from the PLA bone sample tested in the torque device designed and

manufactured. Figure 12 is the equivalent (von-Mises) stress -degree graph obtained as a result of FEA.

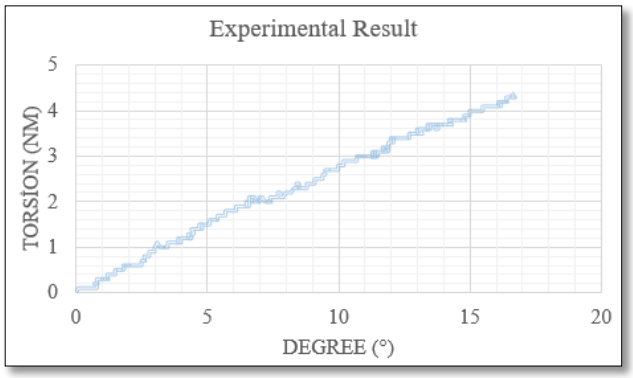

Figure 11. Graphical representation of experimental result

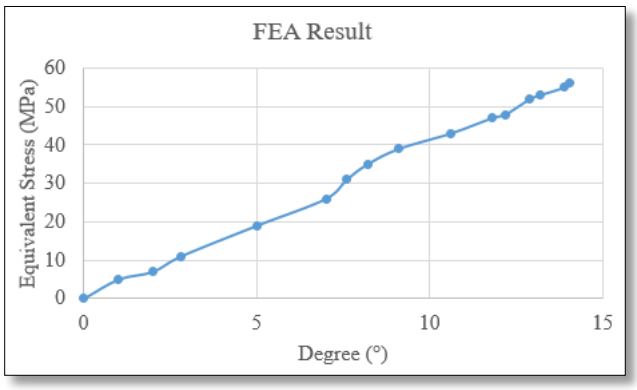

Figure 12. Graphical representation of FEA result

4. CONCLUSION

With this design and manufacture, torsion tests of shapeless and small metatarsal bone have been carried out. The parts of the designed test setup were produced by using a 3D printer. For this purpose, the strength of the designed parts was evaluated firstly by using the FEA, then the production of the parts was carried out according to the FEA results. Torsion test was applied to the first metatarsal bone on the developed device and FEA. The similarity in the obtained graphical results proved that the system works correctly. The first metatarsal bone specimen has undergone plastic deformation in the experiment. The obtained equivalent (von-Mises) stress values from FEA also indicate plastic deformation.

ACKNOWLEDGEMENT

This work is supported by the Scientific Research Projects Unit of Kocaeli University under project no FHD-2020-2143.

AUTHOR CONTRIBUTIONS

Zeliha COŞKUN : Performed the experiments, analyse the results and wrote manuscript. **Talip ÇELİK:** Performed the experiments and analyse the results. **Yasin KİŞİOĞLU:** Analyse the results.

Conflict of interest

There is no conflict of interest in this study.

REFERENCES

Abutahoun I, Ha Jung-Hong, Kwak S & Kim Hyeon-Cheol (2018). Evaluation of dynamic and static torsional resistances of nickel-titanium rotary instruments. Journal of dental sciences.

Ağın B, Çelik T & Kişioğlu Y (2019). Gezen Tavuklar İle Çiftlik Tavuklarinin Femur Kemiklerinin Mekanik Özelliklerinin Belirlenmesi Ve Karşilaştirilmasi.2. Uluslararasi Erciyes Bilimsel Araştirmalar Kongresi

Çelik T, Mutlu İ, Özkan A & Kişioğlu Y (2017). The effect of cement on hip stem fixation: a biomechanical study. *Australasian physical & engineering sciences in medicine*, *40*(2), 349- 357.

Dahl K A, Moritz N & Vallittu P K (2018). Flexural and torsional properties of a glass fiber-reinforced composite diaphyseal bone model with multidirectional fiber orientation. Journal of the Mechanical Behavior of Biomedical Materials, 87, 143-147.

Fatihhi S J, Rabiatul A A R, Harun M N, Kadir M R A, Kamarul T & Syahrom A (2016). Effect of torsional loading on compressive fatigue behaviour of trabecular bone. Journal of the mechanical behavior of biomedical materials, 54, 21-32.

Kaur M & Singh K (2019). Review on titanium and titanium based alloys as biomaterials for orthopaedic applications. *Materials Science and Engineering: C*, 102, 844-862.

Kasra M & Grynpas M D (2007). On shear properties of trabecular bone under torsional loading: effects of bone marrow and strain rate. Journal of Biomechanics, 40(13), 2898-2903.

Kaygusuz B, Ozerinç S (2019). 3 Boyutlu Yazıcı ile Üretilen PLA Bazlı Yapıların Mekanik Özelliklerinin İncelenmesi. Makina Tasarım ve İmalat Dergisi, 1-6.

Kirthana S, Supraja M B, Vishwa A S N & Mahalakshmi N (2020). Static structural Analysis on Femur Bone Using Different Plate Material. Materials Today: Proceedings, 22, 2324-2333.

Kumar K N, Griya N, Shaikh A, Chaudhry V & Chavadaki S (2020). Structural analysis of femur bone to predict the suitable alternative material. Materials Today: Proceedings, 26, 364-368.

Kumar S, Nehra M, Kedia D, Dilbaghi N, Tankeshwar K & Kim K H (2020). Nanotechnology-based biomaterials for orthopaedic applications: Recent advances and future prospects. Materials Science and Engineering: C, 106, 110154.

Kuwashima U, Takeuchi R, Ishikawa H, Shioda M, Nakashima Y & Schröter S (2019). Comparison of torsional changes in the tibia following a lateral closed or medial open wedge high tibial osteotomy. The Knee, 26(2), 374-381.

Murakami Y. (2019), Torsional fatigue. Metal Fatigue (Second Edition), 317-340.

Rohlmann A, Pohl, D & Bender A, Graichen F & Dymke J & Schmidt H & Bergmann G (2014). Activities of

Everyday Life with High Spinal Loads. PloS one. 9. e98510. 10.1371/journal.pone.0098510.

Sykaras N, Iacopino A M, Marker V A, Triplett R G & Woody R D (2000). Implant materials, designs, and surface topographies: their effect on osseointegration. A literature review. International Journal of Oral & Maxillofacial Implants, 15(5).

Traphöner H, Clausmeyer T & Tekkaya A E (2018). Material characterization for plane and curved sheets using the in-plane torsion test–An overview. Journal of Materials Processing Technology, 257, 278-287.

Varghese B, Short D, Penmetsa R, Goswami T & Hangartner T (2011). Computed-tomography- based finite-element models of long bones can accurately capture strain response to bending and torsion. Journal of biomechanics, 44(7), 1374- 1379.

Wahab A H A, Wui N B, Kadir M R A & Ramlee M H (2020). Biomechanical Evaluation of Three Different Configurations of External Fixators for Treating Distal Third Tibia Fracture: Finite Element Analysis in Axial, Bending and Torsion Load. Computers in Biology and Medicine, 104062.

Wu Z, Wu Y, Fahmy M (2020) Shear and torsional strengthening of structures. Structures Strengthened with Bonded Composites, 315- 386, 2020.